

PSFC/JA-00-32

**Signature of Turbulent Zonal Flows
Observed in the DIII-D Tokamak**

Coda, S.,* Porkolab, M.,
Burrell, K.H.**

October 2000

Massachusetts Institute of Technology
Plasma Science and Fusion Center
Cambridge, MA 02139 USA

*Present and permanent address:
Centre de Recherches en Physique des Plasmas
Ecole Polytechnique Fédérale de Lausanne
CH-1015 Lausanne, Switzerland

**General Atomics
PO Box 85608
San Diego, CA 92186-5608

Published in *Physics Letters A*, Vol. 273, p. 125, 2000.

This work supported by the U.S. Department of Energy Contract No. DE-FG02-91ER54109
and Contract No. DE-AC03-89ER51114.

Signature of Turbulent Zonal Flows Observed in the DIII-D Tokamak

Coda, S.*; Porkolab, M.
Massachusetts Institute of Technology
Plasma Science and Fusion Center
Cambridge, MA 02139 USA

Burrell, K.H.
General Atomics
P.O. Box 85608
San Diego, CA 92186-5608

ABSTRACT

The spectrum of turbulent density fluctuations at long poloidal wavelengths in the edge plasma of the DIII-D tokamak peaks at nonzero radial wave number. The associated electric-potential fluctuations cause sheared $\tilde{E} \times B$ flows primarily in the poloidal direction. These *zonal flows* have been predicted by theory and are believed to regulate the overall level of turbulence and anomalous transport. The quantitative features of the measured spectra are in good agreement with predictions.

Controlled nuclear fusion relies on the efficient confinement of high-temperature plasmas. In tokamaks, the confinement provided by the magnetic-field topology is opposed by outward transport, due to Coulomb collisions and plasma instabilities. While researchers have devised ways to control destructive, large-scale magnetohydrodynamic instabilities, small-scale turbulence is generally present at a level that is sufficient to cause some degree of anomalous transport. However, techniques have also been developed to reduce turbulence and have resulted in the steady improvement of tokamak confinement [1]. Parallel advancements in fluctuation measurement techniques, especially noninvasive imaging diagnostics [2], and in the computing power available to numerical simulations [3] have been equally noteworthy and are constantly providing new insight in the properties of turbulence, one of the remaining unsolved problems of classical physics.

The process of turbulence decorrelation and suppression by the sheared $\mathbf{E} \times \mathbf{B}$ flow associated with sheared equilibrium radial electric fields, now well understood theoretically [4], has been identified experimentally as a crucial mechanism in a variety of enhanced-confinement regimes [5]. More recent theoretical and computational work [3,6-11] has led to the important realization that fluctuating sheared poloidal $\mathbf{E} \times \mathbf{B}$ flows, known as zonal flows [12] or radial modes [7], can be driven by microinstabilities and in turn act to regulate them through the same shear stabilization mechanism. In *all* regimes, therefore, plasma turbulence is expected to be in a self-organized state mediated by zonal flows.

Direct experimental observation of zonal flows is expected to be arduous [13], as it would require extracting the components of the velocity field or electric potential with the required long toroidal and poloidal wavelengths. In this Letter, we present the first measurement of the fluctuating plasma density in the relevant region of the spectrum. The measurement was performed with a phase-contrast imaging (PCI) diagnostic [14] in the edge region of the Doublet III-D (DIII-D) tokamak [15]. It is shown that the measured component is characterized by a finite average radial wavelength of the magnitude predicted by theory. The adiabatic-electron constraint then implies the existence of electric-potential fluctuations giving rise to turbulent, sheared, primarily poloidal $\mathbf{E} \times \mathbf{B}$ flows. The estimated zonal flow shear is found to be comparable to the macroscopic $\mathbf{E} \times \mathbf{B}$ shear measured in the high-confinement mode (H-mode) [16], and can thus be expected to have a strong regulating effect.

The PCI diagnostic [17] measures the vertical line integrals of the density fluctuations at 8 locations distributed along a major radius with a uniform adjustable spacing (typically 0.3 to 0.5 cm) and situated in the outer plasma edge of DIII-D (the outermost 10–20% in poloidal magnetic flux). The measurement accesses frequencies in the range 8–1000 kHz with a sensitivity of $\tilde{n}_e \sim 10^{15} \text{ m}^{-3}$.

Owing to the vertical line integration, the PCI measurement is only sensitive to horizontal wave vectors. The toroidal component k_ϕ is known to be negligibly small [18]. Since in the edge region the poloidal projection of the field lines is nearly vertical, a horizontal wave vector is primarily radial, with only a small poloidal component k_θ [19], as illustrated in Fig. 1(a). Thus, the measured spectrum closely approximates the radial spectrum $S(k_r)|_{k_\theta \sim 0, k_\phi \sim 0}$. Extensive analytical and numerical modeling with realistic turbulence spectra [17,19,20] has confirmed this conclusion. A numerical calculation of the responsivity of the system in (k_r, k_θ) space for a typical DIII-D discharge yields the contour plot shown in Fig. 1(b), with the expected anisotropy $|k_r| \gg |k_\theta|$.

To elucidate the spatial structure of the turbulence we examine the spatial correlation function of the PCI signals. This complex Hermitian function, constructed by taking the equal-time correlation coefficient as the real part and its Hilbert transform as the imaginary part, is almost invariably wavelike with a finite spatial period, and decays spatially over a finite decay length [17], as shown in Fig. 2. This is true in Ohmic, low-confinement (L-mode), and high-confinement (H-mode) regimes, in a wide range of plasma parameters, and both inside and outside the last closed flux surface (LCFS). The real part is generally larger than the imaginary part, revealing the coexistence of counter-propagating modes, which are statistically uncorrelated, as evidenced by the lack of peaks and nodes in the signal amplitude.

The wave-number spectrum is obtained by Fourier-transforming the spatial correlation function and dividing the result by the instrumental transfer function. Spatial antialiasing filtering is effected at the hardware level. Several methods for sparse Fourier transforms have been compared and have yielded similar results, insuring the robustness of the calculated spectra [17]. The spectrum derived from the data of Fig. 2 is shown in Fig. 3. The spectrum is always double-peaked, with the two peaks at approximately symmetric positive and negative values. Although predominantly inward propagation was initially reported [19], a broader statistical investigation has shown that there can be imbalance in either the inward or outward direction depending on the discharge.

The value of $|k_r|$ at the peaks, $k_{0r} \neq 0$, which constitutes the key feature of these spectra, can vary between 2 and 7 cm^{-1} and is well above the instrumental cutoff ($1/e$ point at 0.65 cm^{-1}). The frequency spectrum is monotonically decreasing and k_{0r} increases with frequency (see Fig. 4). The average group velocity $\partial\omega/\partial k_{0r}$ is subsonic: typical values are in the range 1.5–4 km/s in Ohmic and L-mode plasmas, but may extend up to 20 km/s in H-mode.

We have carried out specific simulations to test the interpretation of the observed maxima as nonzero- k_r peaks in the $S(k_r)|_{k_\theta \sim 0}$ spectrum [17,19]. In particular, we have attempted to reproduce the measured spectra by postulating a turbulence spectrum peaking at $k_r = 0$ and $k_\theta \neq 0$, as generally found by other measurements [18,21,22]. Because of the strongly anisotropic responsivity of PCI [cf. Fig. 1(b)], this is possible only by assuming at once a large ratio (> 3) of poloidal to radial correlation lengths, a broad $S(k_\theta)$ spectrum with finite energy at $k_\theta = 0$, and varying degrees of up-down spatial asymmetry to explain the variation in directionality. However, even under these conditions we could not generate peaks at $k_r \neq 0$ at all the radial locations covered by the measurement; also, in up-down asymmetric configurations (single-null diverted plasmas), the calculated locations of the positive and negative peaks are not symmetric. By contrast, the proposed interpretation is consistent with all observations.

Electric-potential fluctuations with $k_\theta \sim 0$ and $k_r \neq 0$ have been predicted by theory [11,12,23] to be nonlinearly generated by drift waves in an inverse cascade to long poloidal scale lengths. Lacking a radial component, these zonal flows do not cause cross-field transport. Their importance lies in their ability to limit the radial size of the drift-wave eddies through the shear decorrelation mechanism [4] and hence, effectively, to regulate turbulent transport. After zonal flows were properly included in gyrofluid [6,7,9] and gyrokinetic [3,8,9] simulations, it was found that the predicted transport rates decreased by up to a factor of 10. While this work has focused mainly on the Ion Temperature

Gradient (ITG) mode as the instability drive, which is expected to be dominant in the plasma core, there are also indications [10,13,24] that similar effects should be active in the plasma edge, where resistive ballooning physics may dominate.

The relation between fluctuations in the potential ϕ and in the density n_e , in the collisional plateau and Pfirsch-Schlüter regimes [25] characteristic of these edge plasmas, is given by the adiabatic electron response [6],

$$\tilde{n}_e/n_e = e[\tilde{\phi} - (\tilde{\phi})_{m=0,n=0}]/T_e, \quad (1)$$

where e is the electron charge, T_e is the electron temperature, and m and n are the poloidal and toroidal mode numbers, respectively. Thus, the \tilde{n}_e spectrum should be identical to the $\tilde{\phi}$ spectrum with the exclusion of the component that is exactly uniform azimuthally and poloidally. An example of the evolved $\tilde{\phi}$ spectrum $S(k_r, k_\theta)$ from a gyrofluid code [7] is shown in Fig. 5; the scale lengths here are normalized to ρ_s , the ion sound gyroradius. Superimposed on the contours is the region to which the PCI diagnostic is sensitive [cf. Fig. 1(b)], for typical edge plasma conditions ($\rho_s = 0.15$ cm). This figure shows that our system is sensitive to the radial modes but not to the larger finite- k_θ instability drive. By contrast, measurements by other diagnostics integrate over a broad k_θ range and should find a maximum at $k_r = 0$. This is indeed the case for the majority of tokamak turbulence spectra reported in the literature [18,21,22]. There is therefore no contradiction between those measurements and the present ones.

Predictions for the value of $k_{0r}\rho_s$ vary from 0.1 [13] to 0.6 [7]. In our dataset, this parameter varies between 0.2 and 0.4. Also, recently reported gyrokinetic and gyrofluid zonal-flow frequency spectra have $1/e$ spectral half-widths at $k_r = k_{0r}$ of, respectively, $\Delta f \simeq 4 \times 10^{-4} f_{ci}$ [13], where f_{ci} is the ion cyclotron frequency, and $\Delta f \simeq 10^{-2} v_{ti}/L_n$ [26], where v_{ti} is the ion thermal velocity and L_n is the density gradient scale length [27]. In a set of L-mode plasmas we obtained values of 6 kHz and 7–13 kHz, respectively, for these half-widths, to be compared with experimental values in the range 8–15 kHz [17]. In addition, gyrofluid simulations show that the frequency width is an increasing function of k_r [26], in agreement with our results (cf. Fig. 4). However, such quantitative comparisons may be premature, as numerical work has focused primarily on the plasma core region and on the ITG drive.

Next, we address the issue of the magnitude of the zonal-flow shear. From Eq. 1 we can write $e\tilde{\phi}_{\text{rms}}/T_e > \tilde{n}_{e,\text{rms}}/n_e$. The inequality may be a strong one, as \tilde{n}_e is only affected by the sidebands of the dominant $m=0, n=0$ component of the modes [6,7]; we are not aware at present of any numerical calculations of the magnitude of the sidebands (to lowest order, the ballooning $m=\pm 1$ components). Combining PCI estimates of \tilde{n}_e with density and temperature measurements by Thomson scattering [17], we can establish an approximate lower bound $\tilde{\phi}_{\text{rms}} > 10$ V. We then obtain for the zonal-flow shear $dv_{\mathbf{E}\times\mathbf{B}}/dr = ck_{0r}^2\tilde{\phi}_{\text{rms}}/B > 2 \times 10^5 \text{ s}^{-1}$. This lower bound is within an order of magnitude of the value of the macroscopic, steady-state shear measured in H-mode [16], believed to be responsible for the dramatic transport suppression that accompanies the L–H transition.

One of the key questions about the dynamics of zonal flows concerns the relative roles played by collisionless and collisional processes, as well as nonlinear effects, in damping the flows [28,29]. In the relatively collisional plasma edge the collisionless time scale given by the reciprocal of the magnetic pumping rate [25] ($\sim 35\text{--}55 \mu\text{s}$) is close to the collisional time

scale $1.5 \epsilon \tau_{ii}$ [29] ($\sim 50\text{--}150 \mu\text{s}$), where ϵ is the inverse aspect ratio r/R and τ_{ii} is the ion-ion collision time. The measured decorrelation time of the turbulence lies in the range $20\text{--}40 \mu\text{s}$; however, the instrumental lack of access to frequencies below 8 kHz may cause this quantity to be underestimated by the measurement. Thus, our data are compatible with both collisionless and collisional damping processes. The decorrelation time τ_d increases indefinitely with the radial scale length, as indicated by the function $\tau_d(k_r)$, which is well approximated by a power law $\tau_d \propto k_r^{-\alpha}$ with $1 \leq \alpha \leq 1.5$, as shown in Fig. 6. This result is in agreement with gyrofluid simulations [30].

Nonlinear effects have been predicted to cause a bursting behavior in the zonal flows over a time scale $1.5 \epsilon \tau_{ii}$ [29]. The probability distribution function of the PCI signals is nearly invariably Gaussian for time scales up to 50 ms, whereas an increasingly leptokurtic character (kurtosis > 3) is apparent for intervals exceeding 50 ms, with an asymptotic kurtosis $K \simeq 5.5$ [17]. While the latter can be indicative of intermittent behavior, this occurs over a time scale at least two orders of magnitude larger than that predicted by this theory.

In conclusion, the first study of turbulence in the long-poloidal-wavelength region of the spectrum in the outer edge of DIII-D has led to the first observation of the characteristic spectral signature of zonal flows. These flows have been predicted by theory and are believed to be the chief regulating mechanism for turbulent transport in tokamaks. The results presented here are consistent with most theoretical predictions. However, further numerical simulations specific to edge conditions are required for a more quantitative comparison.

The authors wish to thank the DIII-D team for the operation of the tokamak, heating systems, and diagnostics. Fruitful discussions with M. A. Beer, T. S. Hahm, and R. E. Waltz are gratefully acknowledged. This work was supported by the U.S. Department of Energy under Grant No. DE-FG02-91ER54109 and Contract No. DE-AC03-89ER51114.

REFERENCES

- * Present and permanent address: Centre de Recherches en Physique des Plasmas, Ecole Polytechnique Fédérale de Lausanne, CH-1015 Lausanne, Switzerland.
Email address: Stefano.Coda@epfl.ch
- [1] See B. A. Carreras, *IEEE Trans. Plasma Sci.* **25**, 1281 (1997), and references therein.
 - [2] N. Bretz, *Rev. Sci. Instrum.* **68**, 2927 (1997).
 - [3] Z. Lin *et al.*, *Science* **281**, 1835 (1998).
 - [4] H. Biglari, P. H. Diamond, and P. W. Terry, *Phys. Fluids B* **2**, 1 (1990); T. S. Hahm and K. H. Burrell, *Phys. Plasmas* **2**, 1648 (1995).
 - [5] K. H. Burrell, *Science* **281**, 1816 (1998).
 - [6] G. W. Hammett *et al.*, *Plasma Phys. Control. Fusion* **35**, 973 (1993); M. A. Beer, Ph.D. Thesis, Princeton University, 1994.
 - [7] R. E. Waltz, G. D. Kerbel, and J. Milovich, *Phys. Plasmas* **1**, 2229 (1994).
 - [8] A. M. Dimits *et al.*, *Phys. Rev. Lett.* **77**, 71 (1996).
 - [9] G. Rewoldt *et al.*, *Phys. Plasmas* **5**, 1815 (1998).
 - [10] B. N. Rogers, J. F. Drake, and A. Zeiler, *Phys. Rev. Lett.* **81**, 4396 (1998).
 - [11] P. H. Diamond *et al.*, in *Proceedings of the 17th IAEA Fusion Energy Conference, Yokohama, 1998* (International Atomic Energy Agency, Vienna, Austria, 1999), vol. 4, p. 1421; L. Chen, Z. Lin, and R. White, *Phys. Plasmas* **7**, 3129 (2000).
 - [12] A. Hasegawa, C. G. MacLennan, and Y. Kodama, *Phys. Fluids* **22**, 2122 (1979).
 - [13] T. S. Hahm *et al.*, *Plasma Phys. Control. Fusion* **42**, A205 (2000).
 - [14] S. Coda, M. Porkolab, and T. N. Carlstrom, *Rev. Sci. Instrum.* **63**, 4974 (1992).
 - [15] J. L. Luxon and L. G. Davis, *Fusion Technol.* **8**, 441 (1985).
 - [16] K. H. Burrell, *Phys. Plasmas* **4**, 1499 (1997).
 - [17] S. Coda, Ph.D. Thesis, Massachusetts Institute of Technology, 1997. Available from: http://www.psf.mit.edu/library/rr/97rr013_abs.html (pdf) and <http://theses.mit.edu:80/Dienst/U322.gif> [Accessed September 3, 2000].
 - [18] See P. C. Liewer, *Nucl. Fusion* **25**, 543 (1985), and references therein.
 - [19] S. Coda and M. Porkolab, in *Proceedings of the 21th European Conference on Controlled Fusion and Plasma Physics, Montpellier, 1994* (European Physical Society, Petit-Lancy, Switzerland, 1994), Vol. 1, p. 854.
 - [20] S. Coda and M. Porkolab, *Rev. Sci. Instrum.* **66**, 454 (1995).
 - [21] A. J. Wootton *et al.*, *Phys. Fluids B* **2**, 2879 (1990).
 - [22] R. J. Fonck *et al.*, *Phys. Rev. Lett.* **70**, 3736 (1993).
 - [23] P. H. Diamond and Y. B. Kim, *Phys. Fluids B* **3**, 1626 (1991).
 - [24] B. A. Carreras, V. E. Lynch, and L. Garcia, *Phys. Fluids B* **3**, 1438 (1991).
 - [25] S. P. Hirshman and D. J. Sigmar, *Nucl. Fusion* **21**, 1079 (1981).
 - [26] M. A. Beer and G. W. Hammett, presented at the International Sherwood Fusion Theory Meeting, Los Angeles, 2000 (unpublished).
 - [27] The different normalization factors f_{ci} and v_{ti}/L_n were chosen for the convenience of the respective authors and no fundamental relationship between them is implied.
 - [28] M. N. Rosenbluth and F. L. Hinton, *Phys. Rev. Lett.* **80**, 724 (1998); F. L. Hinton and M. N. Rosenbluth, *Plasma Phys. Control. Fusion* **41**, A653 (1999).
 - [29] Z. Lin *et al.*, *Phys. Plasmas* **7**, 1857 (2000).
 - [30] M. A. Beer and G. W. Hammett, presented at the 39th Annual Meeting of the Division

FIGURES

FIG. 1. (a) Decomposition of a horizontal vector into its radial and poloidal components; (b) responsivity of the PCI system as a function of k_r and k_θ (darker areas denote larger values); note the different scales for the two axes.

FIG. 2. Spatial correlation function of PCI signals: real part (circles), imaginary part (triangles), and envelope (solid curve). The 95% confidence level is 0.02. The plot refers to the region between the LCFS and 3 cm inside, for an Ohmic plasma (toroidal magnetic field 2.1 T, plasma current 1.9 MA, line-averaged density $3 \times 10^{19} \text{ m}^{-3}$, Ohmic power 3.5 MW).

FIG. 3. Radial wave-number spectrum for the case of Fig. 2. The shaded area represents the confidence interval. The spectrum is normalized to an integral of unity and is plotted up to the Nyquist spatial frequency. The blank region near $k = 0$ is below the instrumental cutoff.

FIG. 4. Contours of wave-number and frequency spectrum, raised to the power $1/3$ for visual clarity, for the case of Fig. 2. Darker areas denote larger values. Smoothing in the frequency variable was performed over a 10 kHz interval.

FIG. 5. Contour plot of 2D wave-number spectrum of evolved ITG turbulence, generated by a 3D gyro-Landau fluid computer simulation [adapted with permission from R. E. Waltz, G. D. Kerbel, and J. Milovich, *Phys. Plasmas* **1**, 2229 (1994)]; the superposed shaded area represents the spectral region accessed by the PCI system (the boundary is defined by the $1/e$ level of the responsivity).

FIG. 6. Decorrelation time as a function of radial wave number, for the case of Fig. 2. An inverse-power-law fit gives $\tau_d \propto k_R^{-1}$ for this case.

Fig. 1

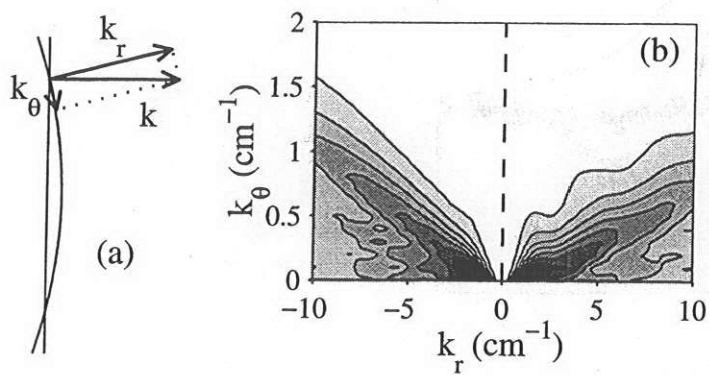


Fig. 2

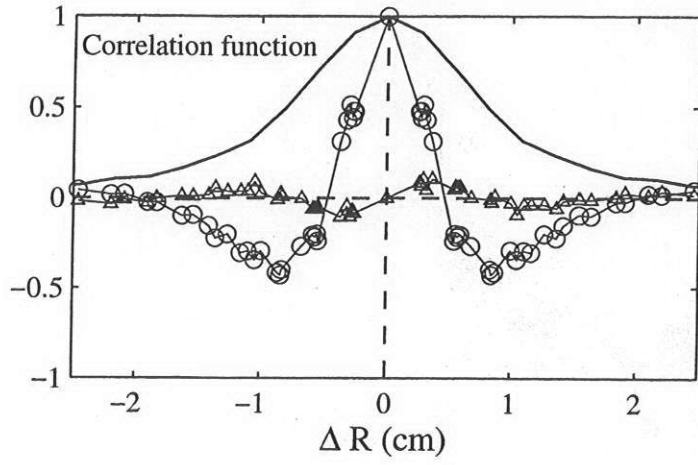


Fig. 3

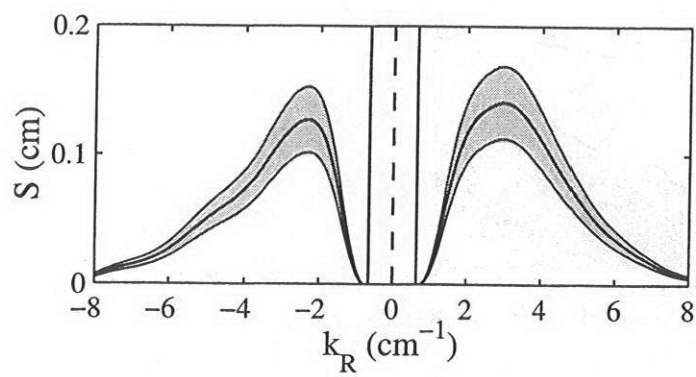


Fig. 4

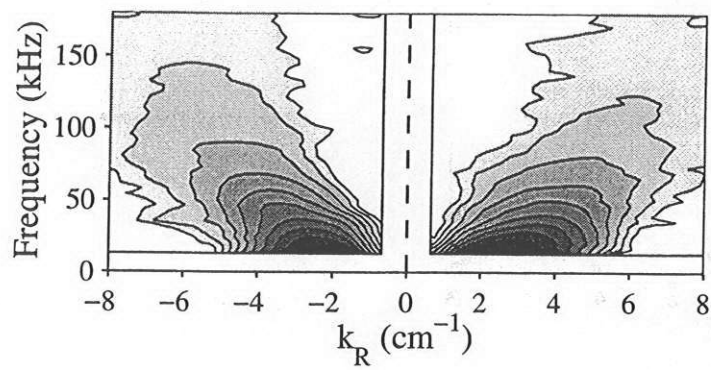


Fig. 5

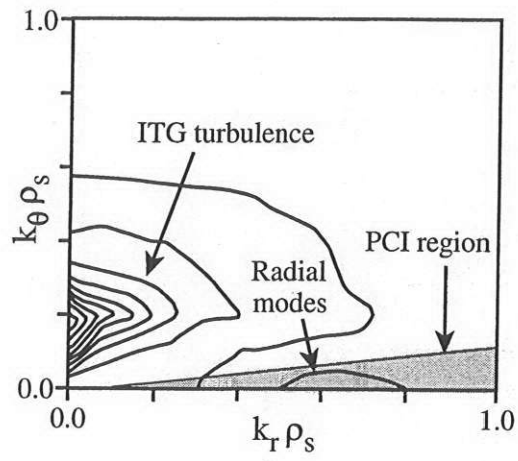


Fig. 6

